Volume 1 | Number 1 | Jan 2013 | Pages 1–100

Journal of
**Materials Chemistry C**
Materials for optical and electronic devices
www.rsc.org/materialsC

ROYAL SOCIETY
OF CHEMISTRY

ROYAL SOCIETY
OF CHEMISTRY

www.rsc.org/materialsC

# Journal of Materials Chemistry C

RSC**Publishing**

## ARTICLE

# Achieving Large Contrast, Low Driving Voltage, and High Stability Electrochromic Device with a Viologen Chromophore

Sheng-Yuan Kao,[a] Yuta Kawahara,[b] Shin'ichi Nakatsuji,[b*] and Kuo-Chuan Ho[a,c*]

Viologen radical salt (VRS), consisting of phenyl viologen (PV) dications and 2,2,6,6-tetramethyl-1-piperidinyloxy derivative (TEMPOD) anions, was successfully synthesized. The VRS was combined with *N,N,N',N'*-tetramethyl-*p*-phenylenediamine (TMPD) to form an electrochromic device (ECD). This ECD offers significant transmittance changes (> 60% at both 580 and 620 nm), but only requires 0.4 V for switching, the lowest driving voltage ever reported. Such a low driving voltage further strengthens the energy-saving capability of the ECD. The incorporation of TEMPOD in the ECD greatly improved its write-erase ability while insufficient bleaching was clearly observed within only 5 cycles in the case of its counterpart without adding TEMPOD anions. No significant decay in the transmittance change was noticed in the proposed ECD after subjecting to 100 cyclings. Even better cycling stability would be expected if counter anions with multiple TEMPO units were utilized.

## Introduction

Electrochromism is a study of reversible color switching in materials upon an application of a dc voltage.[1-3] Due to their ability in controlling light transmission, these materials can be modulated into electrochromic devices (ECDs) that acted as energy-saving smart windows,[4-9] anti-glare rear view mirrors[10] or low power consumption displays.[11-19] Viologens, also known as 1,1'-disubstituted 4,4'-bipyridinium ions, has been proposed as electrochromic materials for several decades due to its high transmittance attenuation.[20-28] 1,1'-diphenyl-4,4'-bipyridinium ions (phenyl viologen, PV) belongs to the viologen family and also exhibits very significant color change.

To further strengthen the energy-saving capability, ECDs with lower driving voltage has recently become the research target. Till today, the potential bias required for most of the ECDs is around 1 ~ 4 V.[29-31] In this work, ECDs that exhibiting extremely low driving voltage of 0.4 V and significant transmittance change (ΔT) are achieved by utilizing PV-based viologen radical salt (VRS) and *N,N,N',N'*-tetramethyl-*p*-phenylenediamine (TMPD).

Conventionally, the working principle of ECDs containing commercial PV(commonly coupled with two chloride anions as a salt, which is denoted as $PVCl_2$ hereafter) and TMPD is shown in **Scheme S1** (Supporting Information). Briefly, the colored species ($PV^{+\bullet}$ and $TMPD^+$) are formed at cathode and anode respectively when an appropriate voltage is applied to the device. After these colored species are formed, they diffuse back to the bulk solution driven by the concentration gradient (**Scheme S1a**). As soon as these two colored species meet in the solution, they recombine and generate colorless viologen dications ($PV^{2+}$) and TMPD. Therefore, when short-circuited, the device would gradually return to the bleached state since the

recombination reaction continues until these colored species are completely consumed (**Scheme S1b**).

Although the viologens like $PVCl_2$ are attractive candidates for electrochromic materials, they often suffer from undesirable/poor write-erase ability or cycling instability resulted from aging process such as side reaction[32] or lack of solubility in their radical cation form.[33] In fact, similar observations were also reported by Fletcher et. al.,[32] Mori et. al.,[34] Kenworthy et. al.[35] when p-cyanophenyl viologen was utilized as the electrochromic material. Generally speaking, PV itself possesses two redox reactions:[36-38]

$$PV^{2+} + e^- \leftrightarrow PV^{+\bullet} \qquad (1)$$
(colorless)  (green)

$$PV^{+\bullet} + e^- \leftrightarrow PV^0 \qquad (2)$$
(green)     (light brown).

However, only the first redox reaction (Eqn. 1) is favored because further reduction (Eqn. 2) would accelerate the aging process through side reaction and crystallization.[39] For example, the undesirable dimer (($PV)_2^{2+}$) can be generated by the following reaction:

$$PV^{2+} + PV^0 \leftrightarrow (PV)_2^{2+} \qquad (3)$$

The side reaction (Eq. 3) is called comproportionation, which has been studied in several literatures.[39-41] The product $(PV)_2^{2+}$ would lead to crystallization which retards the recombination (bleaching) process. In other words, the crystallization damages the ECDs from the viewpoint of long-term stability.[42, 43] Therefore, operating within the first redox couple (Eqn. 1) can alleviate the aging process.

Another aging process in this system is the aggregation of $PV^{+\bullet}$. The $PV^{+\bullet}$ generated upon the reduction tends to aggregate on the ITO electrode due to its lack of solubility (such phenomenon can be observed both in aqueous[33, 43] and non-aqueous solutions[42]). The agglomerate hinders the recombination during the bleaching stage. Therefore, issues like preventing aggregation of $PV^{+\bullet}$ need also to be addressed in order to further improving cycling stability of these ECDs.

Various approaches have been proposed to improve their cycling stability.[20, 39, 44, 45] Nevertheless, very few ECDs simultaneously achieve high optical contrast, low driving voltage, and good cycling stability, which have been the main objectives for many researchers working on electrochromism.

The incorporation of a redox mediator in the ECD is one of the strategies to improve the cycling stability through reducing the formation of $PV^{+\bullet}$ agglomerate. It has been reported that 2,2,6,6-tetramethyl-1-piperidinyloxy (TEMPO) possesses fast, stable, and reversible redox radical center while maintaining high transparency.[46, 47] Moreover, the appropriate formal potential of TEMPO/TEMPO$^+$ moiety[48] further allows it to act as an ideal mediator for the redox reactions of $PV^{+\bullet}/PV^{2+}$ and TMPD/TMPD$^+$ pairs.

Herein, a viologen radical salt (VRS, **Fig. 1**), in which 2,2,6,6-tetramethyl-1-piperidinyloxy derivative (TEMPOD$^-$) serves as the counter anion for the $PV^{2+}$, was synthesized to substitute the commercially available PVCl$_2$. The VRS/TMPD ECD significantly enhances the write-erase ability with a very large transmittance change of greater than 60% at both 580 and 620 nm. Meanwhile, this device requires an extremely low driving voltage of 0.4 V. To our best knowledge, this is the lowest potential bias been reported for driving ECDs. Thus, VRS/TMPD ECD has achieved the main objectives mentioned earlier. The observed low driving voltage would allow the proposed ECD to be integrated with other photovoltaic cells,[49, 50] thus strengthening its energy-saving characteristics.
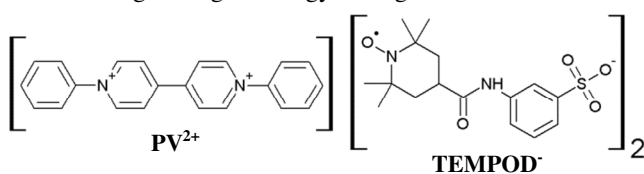


**Fig. 1** Chemical structure of viologen radical salt (VRS).

## Experimental

### Chemicals

TMPD (99%), 2,2,6,6-tetramethyl-1-piperidinyloxy (TEMPO, 98%) and tetrabutylammonium tetrafloroborate (TBABF$_4$, 99%) were purchased from Sigma Aldrich (St. Louis, Missouri, U.S.A.), the solvent Dimethyl sulfoxide (DMSO, > 99.9%) was purchased from J.T. Baker (Center Valley, Pennsylvania, U.S.A.) while PVCl$_2$ (> 97%), 4-carboxy-TEMPO (> 97%), 3-aminobenzenesulfonic acid (> 99%), *N,N'*-dicyclohexylcarbodiimide (DCC, > 98%) and 4-dimethylaminopyridine (DMAP, > 99%) were purchased from Tokyo Chemical Industry (Tokyo, Japan). Tin-doped indium oxide (ITO, Solaronix, Aubonne, Switzerland, R$_{sh}$ = 7 Ω sq$^{-1}$) was used as transparent conducting substrate. All the substrates were cleaned by isopropyl alcohol (IPA) and then subjected to ozone treatment for 20 min before use. The working solution mentioned in the text was sealed between the two ITO substrates with a cell gap of *ca.* 0.06 mm, controlled by one layer of 3M spacer epoxy tape.

### Synthesis of VRS

The viologen radical salt (VRS) is consisted of phenyl viologen dication ($PV^{2+}$) and two 2,2,6,6-tetramethyl-1-piperidinyloxy-derivative anions (TEMPOD$^-$). VRS was synthesized as shown in **Scheme 1**. The preparative procedure is as follows: To a stirred mixture of 4-carboxy-TEMPO (90 mg, 0.45 mmol) and 3-aminobenzensulfonic acid (77 mg, 0.45 mmol) in dichloromethane (20 ml) was added DCC (111 mg, 0.54 mmol) and DMAP (109 mg, 0.90 mmol) and the stirring was continued at an ambient temperature. After 3 days, the reaction was quenched by adding water (20 ml) and stirred for another 10 min. The resulted precipitates were removed by suction under reduced pressure and the dichloromethane layer was separated off. To the water layer was added 1,1'-diphenyl-4,4'-bipyridinium dichloride (71 mg, 0.19 mmol) and stirred for 1 day at an ambient temperature. The resulted brownish solid was isolated by suction under reduced pressure and dried in a desiccator to give brownish yellow powders (113 mg, 60%), whose decomposition temperature was observed to exceed 380 °C. The structure of the product was confirmed by both positive and negative fast atom bombardment mass spectrometry (FAB-MS) measurements: m/z 310 [M$^+$] and m/z 354 [M$^-$]. Besides, the purity of VRS has also been confirmed by the elemental analysis (Found: C, 61.7; H, 6.3; N, 7.9. Calc. for C$_{54}$H$_{62}$N$_6$O$_{10}$S$_2$•2H$_2$O: C 61.58; H 6.12; N 7.98%). The result suggests the existence of some water molecules; this is because a sample of VRS was slightly hygroscopic. For NMR analysis, no clear 1H NMR data for a radical compound can be obtained because of the broadening of absorptions due to the presence of the unpaired electrons on TEMPO moiety. In addition, the insoluble nature of VRS in almost all solvents used for NMR would prevent the measurement. Therefore, NMR analysis of VRS is not included.
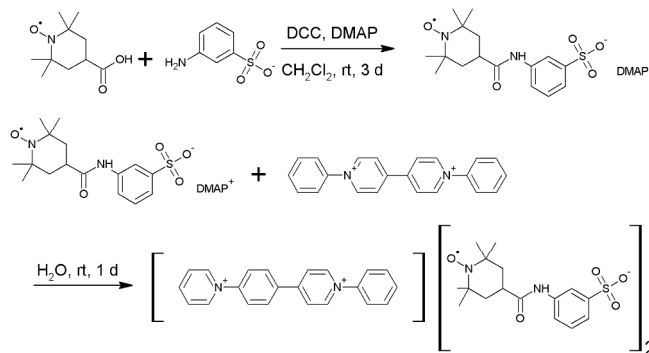


**Scheme 1.** Synthesis route of VRS.

### Fabrication of ECDs

ECDs with various concentration ratios of TMPD and VRS ([TMPD]/[VRS]) were fabricated. The concentration of VRS was fixed to be 0.05 M while that of TMPD was varied to obtain various concentration ratios of TMPD and VRS. In the investigation of TMPD$^+$ reduction, TMPD$^+$ was obtained by oxidizing DMSO solution containing 0.01 M TMPD and 0.1 M TBABF$_4$ using an anodic potential step of 0 V for 1,000 s in a three-electrode system. In this system, ITO, homemade Ag/Ag$^+$ electrode and platinum foil were acted as the working, reference and counter electrode respectively. Other electrochemical analysis of the ECD was performed in a two-electrode system. To obtain VRS at the colored state, the ECD (two-electrode system) containing 0.05 M VRS in DMSO

solution was subjected to 1.0 V bias till redox reaction of VRS reaches steady state.

**Measurements**

Electrochemical measurements were done by a potentiostat/galvanostat (Autolab, model PGSTAT 30, Utrecht, The Netherlands). FAB-MS measurement was obtained by a JEOL AX505 mass spectrometer. Elemental analysis was performed by a Perkin Elmer LS-50B luminescence spectrophotometer. Optical measurements were obtained using a spectrophotometer (Ocean Optics, DH-2000-BAL, Dunedin, Florida, U.S.A.). The sample solution was held in a quartz cell (with a light penetration length of 1 cm) during measurement while the baseline was obtained using an empty quartz cell. In-situ UV-vis spectroscopic data were obtained using the spectrophotometer in conjunction with a potentiostat/galvanostat. The baseline for the in-situ UV-vis data was carried out in air before obtaining the spectroelectrochemical data of the ECDs. The bleaching time ($\tau_b$) and the coloring time ($\tau_c$) are defined as the times required to reach 95% of the maximum transmittance change between the two equilibrium states.

## Results and Discussions

### Electrochromic Working principle of the VRS/TMPD ECD

Electrochemical reactions of VRS include that of $PV^{2+}$ and $TEMPOD^-$. The $PV^{2+}$ exhibits two redox reactions is formulated as Eqn 1 and Eqn 2. On the other hand, the $TEMPOD^-$ in the VRS would provide the following redox reaction:[47, 51]

$$TEMPOD^- \leftrightarrow TEMPOD + e^- \qquad (4)$$
(colorless)    (colorless).

For the anodically coloring material, redox reaction of TMPD can be represented as:[11, 42]

$$TMPD \leftrightarrow TMPD^+ + e^- \qquad (5)$$
(colorless) (dark blue).

    **Scheme 2** shows the working principle of the proposed ECD containing $TEMPOD/TEMPOD^-$, which is modified from that without $TEMPOD/TEMPOD^-$ shown in **Scheme S1**. The $TEMPOD/TEMPOD^-$ redox couple can act as a competitor against $TMPD^+/TMPD$ under the biased condition (**Scheme 2a**) and as a mediator between $PV^{2+}/PV^{+\bullet}$ and $TMPD^+/TMPD$ under the short-circuit condition (**Scheme 2b**).
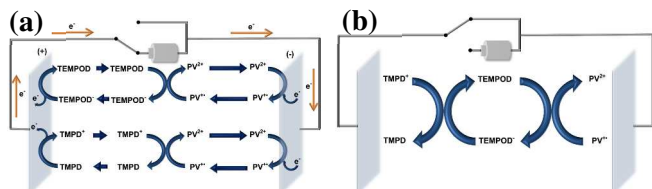


**Scheme 2.** Electrochemical reaction schemes for the proposed ECD (a) showing parallel competing oxidations for $TEMPOD^-$ and TMPD and (b) with TEMPOD redox couple acts as the mediator under the short-circuit condition.

    To verify **Scheme 2b**, UV-Vis characterization was performed. The UV-Vis spectrum of VRS solution (in the absence of $TMPD^+/TMPD$) without applying any potential bias

is presented in **Fig. 2a**. The absence of the characteristic absorption peaks of $PV^{+\bullet}$ at 430 and 715 nm[36] indicates that $PV^{2+}$ and $TEMPOD^-$ are thermodynamically favored. Such phenomenon can also be explained theoretically by the difference in the formal potentials of $TEMPO^+/TEMPO$ and $PV^{2+}/PV^{+\bullet}$. In fact, the formal potential of $TEMPOD^-/TEMPOD$ should be very close to that of $TEMPO^+/TEMPO$ due to the similar chemical structure. The formal potential for the reduction reaction from $TEMPO^+$ to TEMPO was estimated to be 0.48 V (vs. SCE),[48] while the formal potential for the reduction reaction from $PV^{2+}$ to $PV^{+\bullet}$ was estimated to be -0.53 V (vs. SCE).[20] From these reported data, the difference in the standard Gibb's free energy can be calculated to be *ca.* -97.5 kJ mol$^{-1}$. This indicates that electrons transfer from $PV^{+\bullet}$ to $TEMPO^+$ is highly spontaneous. Therefore, electrons transfer from $PV^{+\bullet}$ to TEMPOD to form $PV^{2+}$ and $TEMPOD^-$ should also be spontaneous, which is in good agreement with the result presented in **Fig. 2a**.

    The bleaching reaction of $TMPD^+$ in **Scheme 2b** can be verified by **Fig. 2b**. The colored species $TMPD^+$ gives two iconic absorption peaks at 580 and 620 nm, seen as the solid line of **Fig. 2b**. After adding TEMPO into $TMPD^+$ solution, the colored $TMPD^+$ was effectively reduced to colorless TMPD, as shown in the dashed line of **Fig. 2b**. Because $TEMPOD^-$ is more electron rich than TEMPO, it would be much easier for $TEMPOD^-$ to reduce $TMPD^+$. This result provides evidence that $TEMPOD^-$ tends to be oxidized by $TMPD^+$ to generate TEMPOD, while at the same time, $TMPD^+$ was reduced to colorless TMPD.
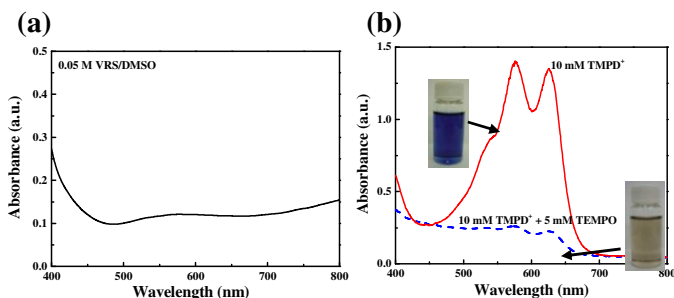


**Fig. 2** (a) UV-Vis spectrum of VRS solution at the short-circuit condition. (b) Absorbance spectra of $TMPD^+$ (colored state TMPD, red solid line) and $TMPD^+$ mixed with TEMPO (blue dashed line). Images of both samples were also included.

### Spectroelectrochemical properties of the VRS/TMPD ECD

    The performance of the ECDs containing various concentration ratios of [TMPD]/[VRS] is listed in **Table S1**. By varying the concentration ratio of [TMPD]/[VRS] from 0.5 to 4.0, it can be seen from **Table S1** that the higher the ratio of [TMPD]/[VRS], the larger the value of the transmittance change ($\Delta T$). If too much TMPD was added in the device ([TMPD]/[VRS] = 6.0), even though the initial $\Delta T$ over 60% can be observed, the bleached state transmittance ($T_b$) dropped dramatically after the second cycle while the colored state transmittance ($T_c$) essentially remained constant (as seen in **Fig. S1**). This is because the excess TMPD would cause facile oxidation reaction at the anode, thus the excess amount of electrons is extracted from the anode and inject to the cathode in a short time. The massive injected electrons flowing to the cathode leads to high concentration of $PV^{+\bullet}$, which tends to form agglomerate on the electrode. In this case, aging process becomes inevitable.

The reason that unequal concentration of TMPD and VRS was observed to perform the best has to do with the competition between TMPD and TEMPOD⁻ anions for oxidation reaction occurred at the anode (seen in **Scheme 1a**). When the potential bias was applied to the device, TEMPOD⁻ is more favorable to migrate to the anode than neutral TMPD molecule. However, since both the reduced and oxidized states of TEMPOD are colorless, the TEMPOD/TEMPOD⁻ pair does not contribute any color change to the ECD. To raise the amount of TMPD being oxidized to its colored state, higher concentration of TMPD was required in the ECD. The optimal concentration ratio was observed at [TMPD]/[VRS] = 4.0. Therefore, only ECD with such condition was subjected to further device characterization.

The variation in absorbance in response to the potential bias (0 to 0.4 V) for the proposed VRS/TMPD is presented in **Fig. 3**. Even though the ECD reaches the darkest state at 0.6 V (as suggest in **Fig. S2a**), it fails to return to the original bleached state if the coloring potential exceeds 0.5 V (**Fig. S2b**). The spectrum in **Fig. S2b** resembles that of $PV^{+\bullet}$ (namely, colored state of VRS, **Fig. S2c**), indicating that the failure of the ECD was mainly resulted from aggregation of $PV^{+\bullet}$. More specifically, an overpotential higher than 0.5 V would lead to vigorous reduction reaction of $PV^{2+}$ and generate high concentration of $PV^{+\bullet}$, which easily forms aggregate on the cathode. The resulting agglomerate therefore retards $PV^{+\bullet}$ from recombining with $TMPD^{+}$, thus resulted in the decrease of write-erase ability.
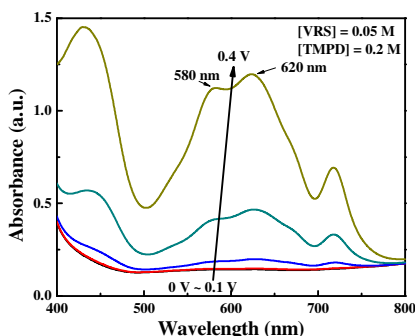


**Fig. 3** The variation in absorbance in response to the potential bias (0 to 0.4 V) for the proposed ECD with [VRS] = 0.05 M and [TMPD] = 0.2 M.

This observation is consistent with that of cyclic voltamograms (**Fig. S3**). **Fig. S3a** shows the cyclic voltammogram of the proposed ECD. With the potential window of 0 ~ 0.4 V, the rise in current density was contributed by the oxidation of TMPD and reduction of $PV^{2+}$. The lack of the cathodic current is expected because the electrons transfer is accomplished through the recombination reaction in the bulk solution, thus no external current can be detected. Namely, the ECD returned to its bleached state as soon as the potential bias was removed. When the potential window was increased to 0 ~ 0.6 V (as seen in **Fig. S3b**), a decay in the anodic peak current was observed after being scanned for 20 cycles. The decay is mainly resulted from the aging process such as aggregation occurred in the ECD, which is consistent with the absorbance spectra noticed in **Fig. S2b**.

If the potential window was further extended to 1.3 V, two redox couples can be observed with poor cycling stability, as shown in **Fig. S3c**. The poor stability presumably is caused by the over-reduction of the $PV^{2+}$ to $PV^{0}$ which would also trigger aging through reactions such as comproportionation (Eqn. 3). The significant aging process leads to huge decay in the peak

current density as noticed in **Fig. S3c**. Therefore, the operating potential window was controlled from 0 to 0.4 V in order to obtain a stable VRS/TMPD ECD. Even though a low driving voltage was applied, a significant ΔT value over 60% at both 580 and 620 nm has been realized.
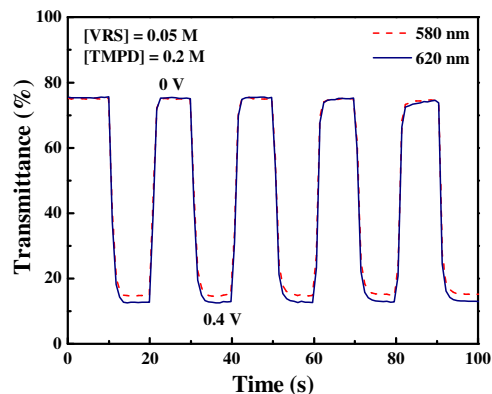


**Fig. 4** The dynamic transmittance (T) curves of an ECD with [VRS] = 0.05 M and [TMPD] = 0.2 M. Both coloring and bleaching intervals are set at 10 s.

**Fig. 4** shows the dynamic transmittance curves of the proposed VRS/TMPD ECD. The performance of this device was quantified and summarized in **Table 1**. The maximum transmittance change of 62.6% was observed at 620 nm, with the bleached state transmittance ($T_b$) of 75.2% and the colored state transmittance ($T_c$) of 12.6%. A significant ΔT of 60.2% can also be observed at another absorption peak of 580 nm with $T_b$ and $T_c$ equal to 75.3 and 15.1% respectively. The bleaching time ($\tau_b$) and the coloring time ($\tau_c$) are within seconds. It is worthwhile to mention here that the driving potential window (0 ~ 0.4 V) is the narrowest one known for ECDs after an extensive literature search.

**Table 1.** The performance of the proposed ECD with [VRS] = 0.05 M and [TMPD] = 0.2 M. The data are summarized from **Fig. 4**.

| Potential window (V) | $\lambda$ (nm) | $T_b$ (%) | $T_c$ (%) | $\tau_b$ (s) | $\tau_c$ (s) | T (%) |
|---|---|---|---|---|---|---|
| 0 ~ 0.4 | 580 | 75.3 | 15.1 | 2.7 | 2.7 | 60.2 |
| 0 ~ 0.4 | 620 | 75.2 | 12.6 | 2.7 | 2.7 | 62.6 |

**Table S2** compares the operating voltage and the electrochromic performance of this work with those of other literatures which also utilized viologen or TEMPO derivatives.[42, 46, 52-58] The ΔT value obtained in this work is comparable to that of others, even though the proposed ECD required the narrowest potential bias.
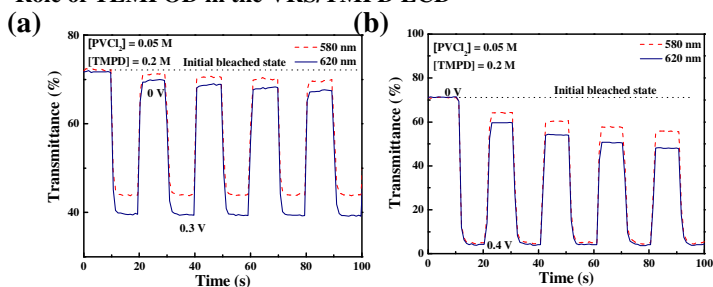
### Role of TEMPOD in the VRS/TMPD ECD



**Fig. 5** The dynamic transmittance curves of an ECD with [PVCl₂] = 0.05 M and [TMPD] = 0.2 M switched between (a) 0 and 0.3 V and (b) 0 and 0.4 V. Both coloring and bleaching intervals are set at 10 s.

To demonstrate enhanced electrochromic behavior of the ECD containing VRS, an ECD consisting of the same electrochromic composition, except VRS is substituted by PVCl$_2$, was fabricated. Undesirable write-erase ability of the device was noticed even within 5 switchings. The UV-Vis spectra of this device at different applied potentials are presented in **Fig. S4a**, in which the characteristic absorption peaks for both PV$^{+\bullet}$ and TMPD$^+$ can also be noticed. Although the absorbance change reached the saturation when the potential bias was increased to *ca.* 0.8 V, the device failed to return to its original bleached state due to its aging effect when the coloring potential reached 0.3 V (as seen in **Fig. S4b**). The dynamic transmittance curves are presented in **Fig. 5a**. Comparing to the proposed ECD containing TEMPOD/TEMPOD$^-$, a smaller ΔT compared to VRS/TMPD ECD at both 580 and 620 nm was observed for the device without TEMPOD/TEMPOD$^-$ when being switched between 0 and 0.3 V. Besides, some undesirable write-erase ability was noticed. The decay in the bleached state transmittance becomes even more severe if the potential bias of 0 to 0.4 V was applied (as seen in **Fig. 5b**)

The enhanced write-erase ability in the VRS/TMPD ECD can be explained as follows. Under the biased potential (**Scheme 2a**), both TMPD$^+$ and TEMPOD that generated at the anode can diffuse to the bulk solution and recombine with PV$^{+\bullet}$. This accelerates the oxidation of PV$^{+\bullet}$ to form PV$^{2+}$, preventing the aggregation of PV$^{+\bullet}$. Under the short-circuit condition (**Scheme 2b**), the reduced TEMPOD (TEMPOD$^-$) reacted with TMPD$^+$ to form TEMPOD, which further reacted with PV$^{+\bullet}$ to form PV$^{2+}$. The propelled oxidation from PV$^{+\bullet}$ to PV$^{2+}$, in the presence of TEMPOD, could prevent PV$^{+\bullet}$ from forming agglomerate. Furthermore, TEMPOD can be regenerated since TEMPOD shows mediator-like behavior. Ultimately, both with and without potential bias would offer the proposed ECD better write-erase ability by reducing the chance of PV$^{+\bullet}$ aggregation on the cathode. This explains why better cycling stability can be achieved in **Fig. 4**, when comparing it with **Fig. 5a** and **Fig. 5b**.

**Fig. 6** presents the stability data of the VRS/TMPD ECD. The dynamic transmittance curves, with the two main absorbance peaks at 580 and 620 nm, were collected for 100 cycles. The coloring interval was set to be 2 s while the bleaching interval was set at 25 s. The facile coloring reaction allows the device to achieve a significant ΔT (> 60%) within 2 s. From **Fig. 6a**, no significant decay in ΔT value was observed at 580 nm after 100 switchings. Similar switching behavior was also observed at 620 nm (**Fig. 6b**). The device was further subjected to the same potential switching for 1,000 times, and it remained 80.2% of its initial ΔT value at 580 nm (**Fig. S5a**). Similarly, the ECD maintained 72.4% of its initial ΔT value at 620 nm after 1,000 cycles (**Fig. S5b**).
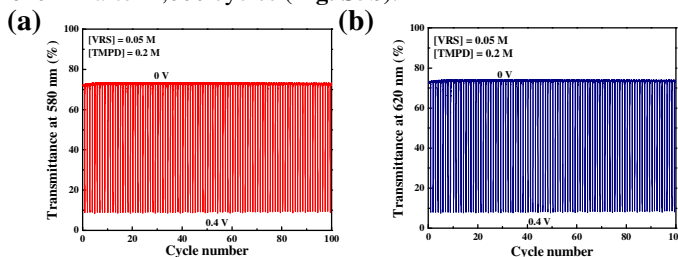
From the results mentioned above, it can be concluded that TEMPOD/TEMPOD$^-$ plays an important role in improving the write-erase ability of the ECD. It is therefore expected that by synthesizing the new counter anions of PV$^{2+}$ having multiple TEMPO units, the ECD with even better cycling stability could be realized.

## Conclusions

In summary, a new ECD consists of VRS and TMPD was successfully fabricated. The resulted device shows high transmittance change (ΔT > 60%) under both 580 and 620 nm while it only requires extremely narrow potential bias of 0.4 V. Such characteristic makes this ECD ideal for energy-saving applications. We have demonstrated, both experimentally and mechanistically, that TEMPOD/TEMPOD$^-$ play an important role in enhancing the write-erase ability. No significant transmittance decay can be observed after switching the proposed ECD for 100 cycles. In fact, this ECD still maintained 80.2 and 72.4% of its initial ΔT after 1,000 switchings at 580 and 620 nm respectively. Therefore, the proposed ECD simultaneously achieved objectives including high ΔT, low driving voltage and good cycling stability. If the counter anions of PV$^{2+}$ with multiple TEMPO units were synthesized, even better cycling stability of the ECD could be expected.

## Acknowledgements

## Notes and references

[a] Department of Chemical Engineering, National Taiwan University, Taipei 10617, Taiwan.

E-mail: kcho@ntu.edu.tw

[b] Department of Material Science, Graduate School of Material Science, University of Hyogo, 3-2-1 Kouto, Kamigori-cho, Ako-gun, Hyogo 678-1297, Japan.

[c] Institute of Polymer Science and Engineering, National Taiwan University, Taipei 10617, Taiwan.

* Corresponding authors: E-mail: kcho@ntu.edu.tw, nakatuji@sci.u-hyogo.ac.jp

† Electronic Supplementary Information (ESI) available: working principle of conventional ECD containing PV and TMPD, variation in absorbance spectra of conventional ECD and proposed ECD, electrochromic performance of ECD with various [TMPD]/[VRS], cyclic voltammograms of VRS/TMPD ECD and long-term cycling stability of VRS/TMPD ECD. See DOI: 10.1039/b000000x/

1. R. J. Mortimer. P. M. S. Monk, D.R. Rosseinsky, *Electrochromism and electrochromic devices*, Cambridge University Press, Cambridge, 2007.
2. C. G. Granqvist, *Handbook of inorganic electrochromic materials*, Elsevier, Amsterdam, 1995.
3. V. K. Thakur, G. Q. Ding, J. Ma, P. S. Lee and X. H. Lu, *Adv. Mater.*, 2012, **24**, 4071.
4. B. P. Jelle, A. Hynd, A. Gustavsen, D. Arasteh, H. Goudey and R. Hart, *Sol. Energy Mater. Sol. Cells*, 2012, **96**, 1.
5. G. A. Niklasson and C. G. Granqvist, *J. Mater. Chem.*, 2007, **17**, 127.

**Fig. 6** The variation in transmittance at (a) 580 and (b) 620 nm as a function of cycle number for the proposed ECD with [VRS] = 0.05 M and [TMPD] = 0.2 M. The ECD was darkened at 0.4 V and bleached at 0 V for the first 100 cycles with a coloring interval of 2 s and a bleaching interval of 25 s.

6. C. G. Granqvist, P. C. Lansaker, N. R. Mlyuka, G. A. Niklasson and E. Avendano, *Sol. Energy Mater. Sol. Cells*, 2009, **93**, 2032.

7. C. G. Wu, M. I. Lu, S. J. Chang and C. S. Wei, *Adv. Funct. Mater.*, 2007, **17**, 1063.

8. D. Ma, G. Shi, H. Wang, Q. Zhang and Y. Li, *J. Mater. Chem. A*, 2014, **2**, 13541.

9. S.-M. Wang, L. Liu, W.-L. Chen, Z.-M. Zhang, Z.-M. Su and E.-B. Wang, *J. Mater. Chem. A*, 2013, **1**, 216.

10. *U.S. Pat.*, 4 917 477, 1990.

11. N. Leventis, M. G. Chen, A. I. Liapis, J. W. Johnson and A. Jain, *J. Electrochem. Soc.*, 1998, **145**, L55.

12. T. Kawata, M. Yamamoto, M. Yamana, M. Tajima and T. Nakano, *Jpn. J. Appl. Phys.*, 1975, **14**, 725.

13. W. Weng, T. Higuchi, M. Suzuki, T. Fukuoka, T. Shimomura, M. Ono, L. Radhakrishnan, H. Wang, N. Suzuki, H. Oveisi and Y. Yamauchi, *Angew. Chem. Int. Ed.,* 2010, **49**, 3956.

14. S. I. Cho, W. J. Kwon, S. J. Choi, P. Kim, S. A. Park, J. Kim, S. J. Son, R. Xiao, S. H. Kim and S. B. Lee, *Adv. Mater.*, 2005, **17**, 171.

15. P. Andersson, R. Forchheimer, P. Tehrani and M. Berggren, *Adv. Funct. Mater.*, 2007, **17**, 3074.

16. A. Cihaner and F. Algı, *Adv. Funct. Mater.*, 2008, **18**, 3583.

17. J. Jensen, A. L. Dyer, D. E. Shen, F. C. Krebs and J. R. Reynolds, *Adv. Funct. Mater.*, 2013, **23**, 3728.

18. H. Jiang, P. Taranekar, J. R. Reynolds and K. S. Schanze, *Angew. Chem. Int. Ed.,* 2009, **48**, 4300.

19. R. Gupta, S. Walia, M. Hosel, J. Jensen, D. Angmo, F. C. Krebs and G. U. Kulkarni, *J. Mater. Chem. A*, 2014, **2**, 10930.

20. C. L. Bird and A. T. Kuhn, *Chem. Soc. Rev.*, 1981, **10**, 49.

21. G. Chidichimo, M. De Benedittis, J. Lanzo, B. C. De Simone, D. Imbardelli, B. Gabriele, L. Veltri and G. Salerno, *Chem. Mat.*, 2007, **19**, 353.

22. R. J. Mortimer and T. S. Varley, *Chem. Mat.*, 2011, **23**, 4077.

23. X. W. Sun and J. X. Wang, *Nano Lett.*, 2008, **8**, 1884.

24. H. C. Ko, M. Kang, B. Moon and H. Lee, *Adv. Mater.*, 2004, **16**, 1712.

25. D. M. DeLongchamp, M. Kastantin and P. T. Hammond, *Chem. Mat.*, 2003, **15**, 1575.

26. H. C. Ko, S. Kim, H. Lee and B. Moon, *Adv. Funct. Mater.*, 2005, **15**, 905.

27. S.-h. Kim, N. Shim, H. Lee and B. Moon, *J. Mater. Chem.*, 2012, **22**, 13558.

28. L. Cao, M. Mou and Y. Wang, *J. Mater. Chem.*, 2009, **19**, 3412.

29. L. Sicard, D. Navarathne, T. Skalski and W. G. Skene, *Adv. Funct. Mater.*, 2013, **23**, 3549.

30. A. Tsuboi, K. Nakamura and N. Kobayashi, *Adv. Mater.*, 2013, **25**, 3197.

31. E. Hwang, S. Seo, S. Bak, H. Lee, M. Min and H. Lee, *Adv. Mater.*, 2014, 5129.

32. S. Fletcher, L. Duff and R. G. Barradas, *J. Electroanal. Chem. Interfacial Electrochem.*, 1979, **100**, 759.

33. H. T. van Dam and J. J. Ponjeé, *J. Electrochem. Soc.*, 1974, **121**, 1555.

34. J. M. Hiroshi Mori, *Jpn. J. Appl. Phys.*, 1987, **26**, 1356.

35. *U.S. Pat.*, 3 712 709, 1990.

36. H. Kamogawa and S. Satoh, *J. Polym. Sci., Part A: Polym. Chem.*, 1988, **26**, 653.

37. H. Kamogawa and S. Sato, *Bull. Chem. Soc. Jpn.*, 1991, **64**, 321.

38. W. W. Porter and T. P. Vaid, *J. Org. Chem.*, 2005, **70**, 5028.

39. R. J. Jasinski, *J. Electrochem. Soc.*, 1977, **124**, 637.

40. P. M. S. Monk, R. D. Fairweather, M. D. Ingram and J. A. Duffy, *J. Chem. Soc., Perkin Trans. 2*, 1992, 2039.

41. P. M. S. Monk, *Dyes Pigment.*, 1998, **39**, 125.

42. K. C. Ho, Y. W. Fang, Y. C. Hsu and L. C. Chen, *Solid State Ion.*, 2003, **165**, 279.

43. N. J. Goddard, A. C. Jackson and M. G. Thomas, *J. Electroanal. Chem. Interfacial Electrochem.*, 1983, **159**, 325.

44. A. Yasuda, H. Mori, Y. Takehana, A. Ohkoshi and N. Kamiya, *J. Appl. Electrochem.*, 1984, **14**, 323.

45. P. M. S. Monk, *J. Electroanal. Chem.*, 1997, **432**, 175.

46. Y. Takahashi, K. Oyaizu, K. Honda and H. Nishide, *J. Photopolym. Sci. Technol.*, 2007, **20**, 29.

47. C.-W. Hu, K.-M. Lee, J.-H. Huang, C.-Y. Hsu, T.-H. Kuo, D.-J. Yang and K.-C. Ho, *Sol. Energy Mater. Sol. Cells*, 2009, **93**, 2102.

48. M. C. Krishna, D. A. Grahame, A. Samuni, J. B. Mitchell and A. Russo, *Proc. Natl. Acad. Sci.*, 1992, **89**, 5537.

49. Z. Xie, X. Jin, G. Chen, J. Xu, D. Chen and G. Shen, *Chem. Commun.*, 2014, **50**, 608.

50. C. Bechinger, S. Ferrere, A. Zaban, J. Sprague and B. A. Gregg, *Nature*, 1996, **383**, 608.

51. F. Geneste, C. Moinet, S. Ababou-Girard and F. Solal, *New J. Chem.*, 2005, **29**, 1520.

52. L. Gao, G. Ding, Y. Wang, Y. Yang, *Appl. Surf. Sci.*, 2011, **258**, 1184.

53. Y. Rong, S. Kim, F. Su, D. Myers and M. Taya, *Electrochim. Acta*, 2011, **56**, 6230.

54. R. Sydam and M. Deepa, *J. Mater. Chem. C*, 2013, **1**, 7930.

55. J. Palenzuela, A. Viñuales, I. Odriozola, G. Cabañero, H. J. Grande and V. Ruiz, *ACS Appl. Mater. Interfaces*, 2014, **6**, 14562.

56. C.-F. Lin, C.-Y. Hsu, H.-C. Lo, C.-L. Lin, L.-C. Chen and K.-C. Ho, *Sol. Energy Mater. Sol. Cells*, 2011, **95**, 3074.

57. R. Sydam, M. Deepa and A. G. Joshi, *Org. Electron.*, 2013, **14**, 1027.

58. Y. Takahashi, N. Hayashi, K. Oyaizu, K. Honda and H. Nishide, *Polym. J.*, 2008, **40**, 763.

# Graphical Abstract

**Achieving Large Contrast, Low Driving Voltage, and High Stability Electrochromic Device with a Viologen Chromophore**

Sheng-Yuan Kao,[a] Yuta Kawahara,[b] Shin'ichi Nakatsuji,[b*] and Kuo-Chuan Ho[a,c*]
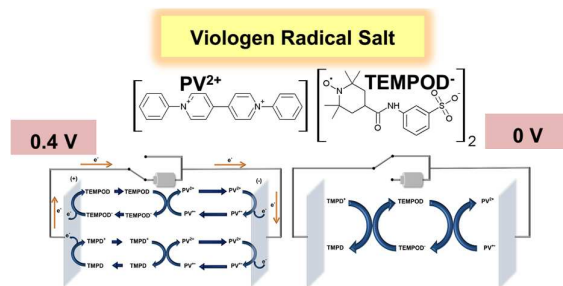
Electrochromic device that utilizes N,N,N',N'-tetramethyl-p-phenylenediamine and viologen radical salt (VRS) exhibits extremely low driving voltage of 0.4 V, high transmittance change (> 60% at 620 nm) and enhanced write-erase ability.